product extracted with pentane. Concentration of the solvent and recrystallization gave 0.090 g (94% yield) of complex **2** identified by comparison with an authentic sample.[2]

FeCp*(η^2-dtc)(PPh_3) (3). A 0.100-g sample of complex **2** (0.295 mmol) and 0.077 g of PPh_3 (0.295 mmol) in 5 mL of ether were photolyzed (visible light) under argon, at room temperature. The reaction followed by IR spectroscopy took 1 h. Ether was removed in vacuo, and the crude product extracted with pentane. Concentration of the solvent and recrystallization gave 0.125 g (80% yield) of complex **3** identified by comparison with an authentic sample.

Acknowledgment. We thank Dr. R. Lapouyade (Université de Bordeaux I) for his kind help in recording photochemical experiments and for very pertinent discussions. The Centre National de la Recherche Scientifique, the University of Bordeaux, the Conseil Régional d'Aquitaine, the National Science Foundation, and the Robert A. Welch Foundation are gratefully acknowledged for financial support.

Registry No. 1, 89875-07-0; 2, 84541-24-2; 3, 119366-44-8.

Supplementary Material Available: Tables of anisotropic thermal parameters of non-hydrogen atoms for complexes 1 and 3 (31 pages); listings of the observed and calculated structure factors for 1 and 3 (32 pages). Ordering information is given on any current masthead page.

Systematic Synthesis, Solution Structural Characterization of the Square-Pyramidal Clusters $MIr_4(CO)_7(\mu\text{-}CO)_2L(\eta^5\text{-}C_5Me_5)(\mu_4\text{-}PPh)$ (M = Rh, Ir; L = CO, PPh_3), and X-ray Structural Determination of the Iridium Derivatives

Rajesh Khattar,[1a] Stephen Naylor,[1b] and Maria D. Vargas*,[1c]

University Chemical Laboratory, Lensfield Road, Cambridge CB2 1EW, U.K.

Dario Braga* and Fabrizia Grepioni

Dipartimento di Chimica "G. Ciamician", Università degli Studi di Bologna, Via Selmi 2, 40126 Bologna, Italy

Received June 23, 1989

The pentanuclear clusters $MIr_4(CO)_9L(\eta^5\text{-}C_5Me_5)(\mu_4\text{-}PPh)$ [L = CO, M = Rh (**3**), Ir (**4**) and L = PPh_2Me or PPh_3, M = Rh (**3a**) or (**3b**), Ir (**4a**) or (**4b**)] are synthesized in good yields by the reactions of $Ir_4(CO)_{11}(PPhH_2)$ and $Ir_4(CO)_{10}(PPhH_2)L$ (L = PPh_2Me or PPh_3), respectively, in acetonitrile with $[M(\eta^5\text{-}C_5Me_5)(NCMe)_3][SbF_6]_2$ (M = Rh, Ir) in the presence of 1,8-diazabicyclo[5.4.0]undec-7-ene (DBU). Compounds **3a**, **3b**, **4a**, and **4b** are also obtained by the reactions of **3** and **4**, respectively, either with L (L = PPh_2Me or PPh_3) in the presence of Me_3NO or with Bu_4NBr to give $[MIr_4(CO)_9Br(\eta^5\text{-}C_5Me_5)(\mu_4\text{-}PPh)]^-$, followed by bromide abstraction with $AgSbF_6$ in the presence of L. All compounds are characterized by fast-atom bombardment mass spectrometry and a combination of ^1H, ^{13}C and ^{31}P NMR. The solid-state structures of **4** and **4b** show that the phosphinidene ligand μ_4 bridges the square base of the square-pyramidal metal atom framework, while the C_5Me_5 is coordinated to one basal Ir atom. The PPh_3 ligand in **4b** replaces an axial CO opposite to the C_5Me_5 group with respect to **4**. Crystal data for **4**: space group $P\bar{1}$, a = 14.511 (5), b = 15.366 (8), c = 13.962 (2) Å, α = 89.99 (3), β = 93.94 (2), γ = 86.15 (3)°, Z = 4. Crystal data for **4b**: space group $P2_1/a$, a = 17.949 (2), b = 9.998 (4), c = 25.606 (5) Å, β = 108.94 (1)°, Z = 4. The solution structures of **3**, **4**, **3b**, and **4b** were determined by low-temperature ^{13}C NMR and are fully consistent with the solid-state structures. For the isostructural compounds **3** and **4** two separate averaging processes are observed at higher temperatures, the first of which has been explained in terms of the formation of the ground-state structure mirror image, complete averaging of all carbonyls occurs at room temperature in these species and also in **3b** and **4b**, whose ^{13}C NMR data did not yield any further mechanistic information.

Introduction

A number of metal carbonyl clusters stabilized by phosphinidene (PR) ligands have been reported during the past few years.[2] Skillfull preparative routes to a range of trinuclear species containing one or even two μ_3-PR ligands have been established;[3] studies of their reactivity have contributed significantly to a better understanding of ligand addition and substitution reactions of metal carbonyl clusters.[4] Recent comparative studies of the reactivity of a number of bis-μ_4-PR square-planar tetranuclear clusters of both the cobalt and iron subgroups could be achieved only as a result of the development of reliable synthetic routes.[5] Such studies have not yet been extended to phosphinidene clusters of nuclearity higher than four, as their isolation has mostly been the result of ser-

(1) Present address: (a) Department of Chemistry and Biochemistry, University of California, Los Angeles, CA 90024; (b) MRC Toxicology Institute, Carshalton, Surrey SM5 4EF, England. (c) Instituto de Quimica, Universidade Estadual de Campinas, C.P. 6154, Campinas 13081, SP, Brazil.

(2) Huttner, G.; Knoll, K. *Angew. Chem., Int. Ed. Engl.* **1987**, *26*, 743.

(3) Huttner, G.; Schneider, J.; Müller, H. D.; Mohr, G.; von Seyerl, J.; Wohlfart, L. *Angew. Chem., Int. Ed. Engl.* **1979**, *18*, 76.

(4) Lunniss, J.; Mac Laughlin, S. A.; Taylor, N. J.; Carty, A. J.; Sappa, E. *Organometallics* **1985**, *4*, 2066.

(5) (a) Vahrenkamp, H.; Wucherer, E. J.; Walter, D. *Chem. Ber.* **1983**, 116, 1219. (b) Müller, E. J. *Angew. Chem., Int. Ed. Engl.* **1981**, *20*, 680.

0276-7333/90/2309-0645$02.50/0

endipity.[6-10] Recent exceptions are the selective preparation of pentanuclear clusters containing μ_4-PR fragments with Os_5, Os_3Ru_2,[11,12] $FeRuCoRh_2$, $FeCo_2Rh_2$, $RuCo_2Rh_2$, Fe_2CoRh_2, and Ru_2CoRh_2[13] frameworks, from the thermal condensation reactions of preformed PR containing trinuclear clusters with metal fragments generated in situ. The chemistry of these species, however, has not been reported.

In this contribution we report details of an alternative systematic synthetic route, that affords the new μ_4-PR-containing clusters $MIr_4(CO)_9L(C_5Me_5)(\mu_4\text{-PR})$, (M = Rh, Ir; L = CO, PPh_2Me, PPh_3), their characterization in solution by ^1H, $^{31}P\{^1H\}$, and ^{13}C NMR and in the solid state, including the X-ray analyses of two pentairidium species and some of their chemistry. A portion of these results has appeared in a preliminary report.[14]

Experimental Section

Materials and Methods. All manipulations and reactions were performed under an atmosphere of dry argon, unless otherwise specified, by using Schlenk-type glassware. Tetrahydrofuran (THF) was dried over sodium and benzophenone; dichloromethane was dried over CaH_2, hexane over sodium, and acetonitrile over phosphorus pentoxide. All solvents were distilled under argon before use.

The progress of the reactions was monitored by analytical thin-layer chromatography (precoated TLC plates, silica gel F-254, 0.25-mm thick, E. Merck). Preparative TLC was carried out in air by using ca. 2-mm-thick glass-backed silica gel plates (20 × 20 cm) prepared from silica gel GF 254 (Type 60, E. Merck).

Infrared (IR) spectra were recorded on a Perkin-Elmer 983 instrument, scanning between 2200 and 1600 cm^{-1}. ^1H, ^{13}C, and ^{31}P NMR data were obtained on Bruker WM 250 or WH 400 instruments by using deuterated solvents as lock and reference [^1H and ^{13}C, $SiMe_4$; ^{31}P, 1% $P(OMe)_3$ in C_6D_6]. $Cr(acac)_3$ (ca. 0.05 M) was added to ^{13}C samples as a relaxation reagent when necessary. Electron impact mass spectra (EI MS, 70 eV) were recorded by using a Kratos MS 12 mass spectrometer. Fast-atom bombardment mass spectra (FAB MS) were obtained on a Kratos MS 50, the atom beam being produced by an Ion Tech FAB gun operating with xenon at 8 kV with a current of 40 μA; *p*-nitrobenzyl alcohol was used as a matrix. All m/z values are referred to ^{193}Ir. $Ir_4(CO)_{12}$,[15] $Ir_4(CO)_{11}L$,[16-18] and $Ir_4(CO)_{10}LL'$ (L = $PPhH_2$, L' = PPh_2Me or PPh_3)[17] and $[M(C_5Me_5)(NCMe)_3][SbF_6]_2$ (M = Rh and Ir)[19] were prepared according to published procedures; all other reagents were purchased from commercial sources. Trimethylamine *N*-oxide dihydrate was sublimed before use, and 1,8-diazabicyclo[5.4.0]undec-7-ene (DBU) was distilled in vacuo. The other reagents were used as supplied.

Preparation of $MIr_4(CO)_{10}(C_5Me_5)(PPh)$ [M = Rh (3), Ir (4)]. A bright red suspension of $Ir_4(CO)_{11}(PPhH_2)$ (60.0 mg, 0.050 mmol) and $[Rh(C_5Me_5)(NCMe)_3][SbF_6]_2$ (45.8 mg, 0.055 mmol) in acetonitrile (15 mL) was left stirring for 15 min and then treated with DBU (8.3 μL, 0.055 mmol), resulting in an instantaneous darkening of the reaction mixture. After 1 h of stirring at 25 °C, the solvent was evaporated in vacuo. Purification by preparative TLC (dichloromethane–hexane, 3:7) afforded $RhIr_4(CO)_{10}(C_5Me_5)(PPh)$ (**3**, 62.0 mg, 0.045 mmol, 89%, R_f 0.42). Recrystallization of the brown solid from dichloromethane–hexane gave an analytically pure sample of **3**. Anal. Calcd for $C_{26}H_{20}O_{10}PRhIr_4$: C, 22.4; H, 1.4. Found: C, 22.2; H, 1.6. IR ν_{CO}(hexane) 2072 (s), 2039 (vs), 2024 (vs), 2009 (vw), 1993 (w), 1981 (w), 1855 (w), 1822 (vw) cm^{-1}; EI MS, m/z 1398 ($M^{\bullet+}$), 1398 − 28x, x = 1–10 ($M - (CO)_x^{\bullet+}$); FAB MS, m/z 1399 ($MH^{\bullet+}$), 1399 − 28x, x = 1–8 ($MH - (CO)_x^{\bullet+}$); ^1H NMR (CD_2Cl_2) δ 1.82 (dd, J_{H-P} = 2.2 Hz, J_{H-Rh} = 0.2 Hz, 15 H, C_5Me_5); $^{31}P\{^1H\}$ NMR (CD_2Cl_2) δ 130.44 (d, J_{P-Rh} = 105.4 Hz, PPh); $^{13}C\{^1H\}$ NMR (CD_2Cl_2, 183 K) δ 100.63 (s, 5 C) and 10.36 (d, J_{C-Rh} = 12.4 Hz, 5 C, C_5Me_5), 128.29 (d, J_{C-P} = 13.8 Hz), 129.87 (d, J_{C-P} = 15.9 Hz), 130.61 (s), and 138.70 (d, J_{C-P} 17.0 Hz, PPh), 166.66 (s, 1, CO), 171.56 (d, J_{C-P} = 48.0 Hz, 1 CO), 174.05 (d, J_{C-P} = 10.9 Hz, 1 CO), 175.11 (d, J_{C-P} = 40.5 Hz, 1 CO), 175.95 (s, 1 CO), 179.82 (s, 1 CO), 184.82 (s, 1 CO), 185.15 (d, J_{C-P} 22.5 Hz, 1 CO), 190.50 (s, 1 CO), 191.42 (d, J_{C-P} 18.8 Hz, 1 CO). The use of dichloromethane (20 mL) instead of acetonitrile in this reaction afforded, after purification on commercial TLC plates, **3** [17.7 mg, 0.012 mmol, 24%], some minor bands which were not characterized, a large base line, and a green compound, formulated as $Ir_8Rh(CO)_{20}(C_5Me_5)(PPh)_2$ (**3x**) (5.8 mg, 0.0027 mml, 9.0% R_f 0.37): IR ν_{CO} (hexane) 2090 (vw, sh), 2085 (w), 2071 (m), 2054 (vs), 2039 (m, sh), 2032 (m), 2025 (s), 2012 (m, sh), 1989 (w), 1849 (w), 1823 (w) cm^{-1}; FAB MS, m/z 2558.

The same procedure was used for the preparation and purification of the dark-brown $Ir_5(CO)_{10}(C_5Me_5)(PPh)$ (**4**, 34.1 mg, 0.023 mmol, 46%, R_f 0.38), except that the corresponding iridium dication species $[Ir(C_5Me_5)(NCMe)_3][SbF_6]_2$ (50.7 mg, 0.055 mmol) was used and the reaction was carried out at 50 °C for 3 h. Recrystallization of the brown solid from dichloromethane–hexane gave an analytically pure sample of **4**. Crystals for the X-ray analysis were obtained from acetonitrile by slow evaporation at 25 °C. Anal. Calcd for $C_{26}H_{20}O_{10}PIr_5$: C, 21.0; H, 1.4. Found: C, 21.2; H, 1.2. IR ν_{CO} (hexane) 2072 (s), 2040 (vs), 2024 (vs), 2010 (vw), 1994 (w), 1981 (w), 1855 (w), 1832 (vw) cm^{-1}; EI MS m/z 1488 ($M^{\bullet+}$), 1488 − 28x, x = 1–10 ($M - (CO)_x^{\bullet+}$); FAB MS, m/z 1489 ($MH^{\bullet+}$), 1489 − 28x, x = 1–8 ($MH - (CO)_x^{\bullet+}$); ^1H NMR (CD_2Cl_2) δ 2.08 (d, J_{H-P} = 1.6 Hz, C_5Me_5); ^{31}P NMR (CD_2Cl_2) δ 60.05 (s, PPh); $^{13}C\{^1H\}$ NMR (CD_2Cl_2, 193 K) δ 90.10 (s, 5 C) and 9.97 (s, 5 C, C_5Me_5), 134.37 (d, J_{C-P} = 11.2 Hz), 130.00 (s), 129.55 (d, J_{C-P} = 10.7 Hz), and 128.76 (d, J_{C-P} = 9.7 Hz, PPh), 167.71 (s, 1 CO), 171.13 (d, J_{C-P} = 10.5 Hz, 1 CO), 172.90 (d, J_{C-P} = 36.0 Hz, 1 CO), 172.98 (d, J_{C-P} = 53.2 Hz, 1 CO), 174.12 (s, 1 CO), 177.61 (s, 1 CO), 178.12 (d, J_{C-P} = 18.2 Hz, 1 CO), 182.57 (s, 1 CO), 184.79 (d, J_{C-P} = 22.0 Hz, 1 CO), 190.64 (s, 1 CO).

The use of dichloromethane (20 mL) instead of acetonitrile in this reaction afforded, after purification on commercial TLC plates, **4** (20.0 mg, 0.013 mmol, 27%, R_f 0.38), five other minor bands with lower R_f's, which were not characterized, a large base line, and a green compound formulated as $Ir_9(CO)_{20}(C_5Me_5)(PPh)_2$ (**4x**, 6.8 mg, 10.0%, R_f 0.35): IR ν_{CO} (hexane) 2090 (vw, sh), 2085 (w), 2072 (m), 2054 (vs), 2040 (m, sh), 2033 (m), 2025 (s), 2012 (m, sh), 1989 (w), 1959 (vw), 1849 (w), 1835 (w), 1826 (w) cm^{-1}; FAB MS, m/z 2648.

Preparation of $MIr_4(CO)_9(PPh_2Me)(C_5Me_5)(PPh)$ [M = Rh (3a), Ir (4a)]. A procedure similar to that used for the syntheses of **3** and **4** was followed to produce **3a** and **4a**. A red suspension of $Ir_4(CO)_{10}(PPh_2Me)(PPhH_2)$ (41.0 mg, 0.030 mmol) and $[Rh(C_5Me_5)(NCMe)_3][SbF_6]_2$ (27.5 mg, 0.033 mmol) in acetonitrile (10 mL) was left stirring for 15 min and then treated with DBU (9.9 μL, 0.066 mmol), resulting in an instantaneous darkening of the reaction mixture. After 1 h of stirring at 25 °C, the solvent was evaporated in vacuo. Purification by preparative TLC (dichloromethane–hexane, 2:3) afforded $RhIr_4(CO)_9(PPh_2Me)(C_5Me_5)(PPh)$ (**3a**, 35.1 mg, 0.023 mmol, 76%, R_f 0.45). Minor bands were observed on the TLC plates but were not characterized. Recrystallization of the dark-brown solid from

(6) Fernandez, J. M.; Johnson, B. F. G.; Lewis, J.; Raithby, P. R. *J. Chem. Soc., Dalton Trans.* **1981**, 2250.
(7) Fernandez, J. M.; Johnson, B. F. G.; Lewis, J.; Raithby, P. R. *Acta Crystallogr.* **1979**, *B35*, 1711.
(8) Mays, M. J.; Raithby, P. R.; Taylor, P. L.; Henrick, K. *J. Chem. Soc., Dalton Trans.* **1984**, 959.
(9) Field, J. S.; Haines, R. J.; Smit, D. N. *J. Chem. Soc., Dalton Trans.* **1988**, 1315.
(10) Natarajan, K.; Zolnai, L.; Huttner, G. *J. Organomet. Chem.* **1981**, *209*, 85.
(11) Colbran, S. B.; Johnson, B. F. G.; Lewis, J.; Sorrel, R. M. *J. Chem. Soc., Chem. Commun.* **1986**, 525.
(12) Colbran, S. B.; Johnson, B. F. G.; Lahoz, F. J.; Lewis, J.; Raithby, P. R. *J. Chem. Soc., Dalton Trans.* **1988**, 1199.
(13) Mani, D.; Vahrenkamp, H. *Chem. Ber.* **1986**, *119*, 3649.
(14) Braga, D.; Vargas, M. D. *J. Chem. Soc., Chem. Commun.* **1988**, 1443.
(15) Whyman, R. *J. Chem. Soc., Dalton Trans.* **1972**, 2294.
(16) Nicholls, J. N.; Raithby, P. R.; Vargas, M. D. *J. Chem. Soc., Chem. Commun.* **1986**, 1617.
(17) Khattar, R.; Vargas, M. D., manuscript in preparation.
(18) (a) Ros, R.; Canziani, F.; Roulet, R. *J. Organomet. Chem.* **1984**, *267*, C9. (b) Ros, R.; Scrivanti, A.; Albano, V. G.; Braga, D.; Garlaschelli, L. *J. Chem. Soc., Dalton Trans.* **1986**, 2411.
(19) (a) Kang, J. W.; Moseley, K.; Maitlis, P. M. *J. Am. Chem. Soc.* **1969**, *91*, 5970. (b) White, C.; Thompson, S. J.; Maitlis, P. M. *J. Chem. Soc., Dalton Trans.* **1977**, 1654.

dichloromethane–hexane gave an analytically pure sample of **3a**. Anal. Calcd for $C_{38}H_{33}O_9P_2RhIr_4$: C, 29.3; H, 2.1. Found: C, 29.1; H, 2.3. IR ν_{CO} (hexane) 2046 (m), 2021 (vs), 2011 (m, sh), 1992 (m), 1977 (w), 1864 (w), 1811 (m, br) cm^{-1}; EI MS, m/z 1462 $(M - 108)^{\bullet+}$), 1462 – 28x, x = 1–10 (M – Ph – $(CO)_x^{\bullet+}$); FAB MS, m/z 1571 $(MH^{\bullet+})$, 1571 – 28x, x = 1–6 (MH – $(CO)_x^{\bullet+}$), 1436 (MH – 135)$^{\bullet+}$), 1436 – 28x, x = 1–3 (MH – C_5Me_5 – $(CO)_x^{\bullet+}$); ^1H NMR (CD_2Cl_2) δ 1.65 (d, J_{H-P} = 1.6 Hz, 15 H, C_5Me_5), 2.14 (dd, J_{H-P} = 11.5 Hz, J_{H-P} = 1.7 Hz, 3 H, PPh_2Me); ^{31}P NMR (CD_2Cl_2) δ 99.49 (dd, J_{P-Rh} = 163.9 Hz, J_{P-P} = 6.1 Hz, PPh), –146.09 (d, PPh_2Me).

The same procedure was used for the preparation and purification of the olive-green $Ir_5(CO)_9(PPh_2Me)(C_5Me_5)(PPh)$ (**4a**, 33.8 mg, 0.020 mmol, 68%, R_f 0.43), except that the corresponding iridium dicationic species $[Ir(C_5Me_5)(NCMe)_3][SbF_6]_2$ (30.6 mg, 0.033 mmol) was employed and the reaction was carried out at 30 °C for 4 h. Anal. Calcd for $C_{38}H_{33}O_9P_2Ir_5$: C, 27.5; H, 2.0. Found: C, 27.7; H, 2.3. IR ν_{CO} (hexane) 20.48 (m), 2021 (vs), 2012 (m, sh), 1992 (m), 1977 (w), 1965 (w), 1820 (w), 1808 (w) cm^{-1}; EI MS, m/z 1552 (M – 108)$^{\bullet+}$), 1552 – 28x, x = 1–9 (M – Ph – $(CO)_x^{\bullet+}$); FAB MS, m/z 1661 $(MH^{\bullet+})$, 1661 – 28x, x = 1–6 (MH – $(CO)_x^{\bullet+}$), 1528 (MH – 135$^{\bullet+}$), 1528 – 28x, x = 1–3 (MH – C_5Me_5 – $(CO)_x^{\bullet+}$); ^1H NMR (CD_2Cl_2) δ 1.88 (d, J_{H-P} = 1.4 Hz, 15 H, C_5Me_5), 2.15 (dd, J_{H-P} = 10.0 Hz, J_{H-P} = 0.5 Hz, 3 H, PPh_2Me); ^{31}P NMR (CD_2Cl_2) δ 86.48 (s, PPh); –141.35 (s, PPh_2Me).

Reaction of 3 with PPh_3 in the Presence of Me_3NO. No reaction was observed when a dichloromethane (15 mL) solution of $RhIr_4(CO)_{10}(C_5Me_5)(PPh)$ (28 mg, 0.020 mmol) and PPh_3 (5.8 mg, 0.022 mmol) was stirred at room temperature for 24 h. It was then cooled to –50 °C and treated with a dichloromethane (1 mL) solution of sublimed Me_3NO (1.7 mg, 0.022 mmol). The reaction mixture was allowed to warm to room temperature and was left stirring for 1 h. Purification by preparative TLC (as described for **3a**) afforded $RhIr_4(CO)_9(PPh_3)(C_5Me_5)(PPh)$ (**3b**, 30.7 mg, 0.019 mmol, 96.5%, R_f 0.44). The same procedure was followed to produce **3a**, **4a**, and **4b**. **3b**: IR ν_{CO} (hexane) 2046 (m), 2021 (vs), 2011 (m, sh), 1992 (m), 1977 (w), 1864 (w), 1811 (m, br) cm^{-1}; $^{13}C\{^1H\}$ NMR (CD_2Cl_2, 243 K) δ 173.54 (dd, J_{C-P} = 41.9 Hz, J_{C-P} = 10.0 Hz, 1 CO), 176.74 (d, J_{C-P} = 22.8 Hz, 1 CO), 177.82 (d, J_{C-P} = 44.5 Hz, 1 CO), 178.47 (s, 1 CO), 180.63 (s, 1 CO), 182.67 (s, 1 CO), 191.47 (d, J_{C-P} = 8.9 Hz, 1 CO), 195.80 (d, J_{C-P} = 17.6 Hz, 1 CO), 200.40 (d, J_{C-P} = 31.9 Hz, 1 CO). **4b**: IR ν_{CO} (hexane) 2049 (m), 2020 (vs), 2012 (m, sh), 1991 (m), 1976 (w), 1965 (w), 1820 (w), 1805 (w) cm^{-1}; $^{13}C\{^1H\}$ NMR (CD_2Cl_2, 203 K) δ 172.89 (d, J_{C-P} = 15.0 Hz, 1 CO), 174.35 (dd, J_{C-P} = 44.2 Hz, J_{C-P} = 9.1 Hz, 1 CO), 175.12 (s, 1 CO), 176.16 (d, J_{C-P} = 43.0 Hz, 1 CO), 177.70 (s, 1 CO), 180.22 (s, 1 CO), 190.05 (d, J_{C-P} = 6.0 Hz, 1 CO), 190.44 (d, J_{C-P} = 22.9 Hz, 1 CO), 195.01 (d, J_{C-P} = 27.0 Hz, 1 CO).

Reaction of 3 with PPh_3 in the Absence of Me_3NO. Heating **3** (28 mg, 0.020 mmol) with PPh_3 (5.8 mg, 0.022 mmol) in hexane (10 mL) under reflux for 1 h produced, after purification by TLC (as described for **3a**) $RhIr_4(CO)_9(PPh_3)(C_5Me_5)(PPh)$ (**3b**, 4.1 mg, 0.005 mmol, 22.2%), along with unreacted material and decomposition products (base line on the TLC).

Reaction of 4 with (i) $[Bu_4N]Br$ and (ii) PPh_3 and Ag$[SbF_6]$. The reaction of $Ir_5(CO)_{10}(C_5Me_5)(PPh)$ (29.7 mg, 0.020 mmol) and $[Bu_4N]Br$ (7.1 mg, 0.022 mmol) was carried out in THF (10 mL) under reflux for 7 h. The dark-brown product formed was not isolated for full characterization but was formulated as $[Bu_4N][Ir_5(CO)_9Br(C_5Me_5)(PPh)]$ (**4c**): IR ν_{CO} (THF) 2037 (m), 2000 (vs), 1995 (s, sh), 1974 (m), 1968 (m, sh), 1794 (w, br) cm^{-1}. The reaction mixture was cooled to –60 °C; PPh_3 (5.2 mg, 0.020 mmol) and $Ag[SbF_6]$ (7.6 mg, 0.022 mmol) were added as solids. The reaction mixture was allowed to warm to room temperature and was filtered through silica. Evaporation of the solvent and purification by preparative TLC (as described for **3a**) gave the olive-green compound $Ir_5(CO)_9(PPh_3)(C_5Me_5)(PPh)$ (**4b**, 15.4 mg, 0.009 mmol, 42%).

Preparation of ^{13}CO-Enriched $Ir_4(CO)_{12}$. A suspension of $Ir_4(CO)_{12}$ (1 g, 0.905 mmol) and $[Bu_4N]Br$ (0.438 g, 1.358 mmol) in THF (40 mL) was heated under reflux for 1 h. The resulting orange solution of $[Bu_4N][Ir_4(CO)_{11}Br]$[20] was stirred at room temperature under 1 atm of ^{13}CO. after 24 h, the solution had turned pale yellow due to the precipitation of the $Ir_4(^*CO)_{12}$. The suspension was heated under reflux again for 1 h, and the same enrichment procedure was repeated once more. The $Ir_4{}^*CO)_{12}$ enrichment was of the order of 20–25% on the basis of EI MS. The ^{13}C NMR spectrum could not be obtained due to the poor solubility of $Ir_4(CO)_{12}$ in all common organic solvents.

Table I. Crystal Data and Details of Measurements for 4 and 4b

	4	4b
formula	$C_{26}H_{20}Ir_5O_{10}P$	$C_{43}H_{35}Ir_5O_9P_2$
cryst syst	triclinic	monoclinic
space group[a]	$P\bar{1}$	$P2_1/a$
a, Å	14.511 (5)	17.949 (2)
b, Å	15.366 (8)	9.998 (4)
c, Å	13.962 (2)	25.606 (5)
α, deg	89.99 (3)	
β, deg	93.94 (2)	108.94 (1)
γ, deg	86.15 (3)	
V, Å^3	3098.8	4346.3
Z	4	4
d_{calcd}, g cm^{-3}	3.18	2.63
$F(000)$	2623	3119
cryst size, mm	0.12 × 0.15 × 0.10	0.15 × 0.15 × 0.08
μ(Mo Kα), cm^{-1}	207.2	148.1
scan range, deg	$2.5 < \theta < 25$	$2.5 < \theta < 25$
scan method	$\omega/2\theta$	$\omega/2\theta$
scan interval, deg	0.75 + 0.35 tan θ	0.75 + 0.35 tan θ
prescan speed, deg min^{-1}	5	5
prescan acceptance $\sigma(I)/I$	0.5	0.5
required final $\sigma(I)/I$	0.01	0.01
bkgd measurements equal to	peak time	peak time
octants coll	$\pm h,\pm k,\pm l$	$\pm h,+k,+l$
no. of data coll	11 457	7775
no. of data used ($I_o > 2.5\sigma(I_o)$)	6965	4046
R (R_w)	0.050 (0.057)	0.049 (0.052)

[a] The space group assignment was based on systematic absences and confirmed by successful refinement of the structure models.

Preparation of ^{13}CO-Enriched 3, 4, 3b, and 4b. ^{13}CO-enriched samples of **3** and **4** were prepared from ^{13}CO-enriched **1a** and were used for the preparation of samples of **3b** and **4b** by the same procedure as described above.

X-ray Structure Determination. Crystal data for **4** and **4b** are summarized in Table I, together with some experimental details. Both data sets were collected at room temperature on an Enraf-Nonius CAD-4 diffractometer with Mo Kα radiation (λ = 0.71069 Å), reduced to F_o, and corrected for crystal decay. For both crystals no azimuthal scan reflections could be measured. An absorption correction was applied by the Walker and Stuart method[21] once the complete structural models were obtained and all non-hydrogen atoms refined isotropically (correction ranges in ϕ and μ: 0.66–1.00 and 0.50–1.00 for **4** and **4b**, respectively).

Both structures were solved by direct methods, which afforded the positions of all Ir atoms. All C, O, and P atoms were located from subsequent difference Fourier synthesis. The refinements of the structural models were made by least-square calculations, the minimized function being $\sum w(F_o - KF_c)^2$. The weighing scheme employed was $w = K/[\sigma^2(F) + |g|F^2]$, where both K and g were refined (1.0 and 0.0005 for **4** and 2.48 and 0.0008 for **4b**. For all computations the SHELX package of crystallographic programs[22] was used with the analytical scattering, factors corrected for the real and imaginary parts of anomalous dispersion, taken from ref 23.

Anisotropic treatment of the atomic thermal vibrations in **4** was confined to Ir and P atoms, because of the occurrence of several nonpositive definite parameters for the light atoms, probably due to insufficient correction for absorption. All atoms

(20) Chini, P.; Ciani, G.; Garlaschelli, L.; Manassero, M.; Martinengo, S.; Sironi, A.; Canziani, F. *J. Organomet. Chem.* **1970**, *152*, C356.

(21) Walker, N.; Stuart, D. *Acta Crystallogr., Sect. A* **1983**, *39A*, 158.

(22) Sheldrick, G. M. SHELX76, Program for Crystal Structure Determination; University of Cambridge: Cambridge, England, 1976.

(23) *International Tables for X-ray Crystallography*; Kynoch Press: Birmingham, England, 1975; Vol. IV, pp 99–149.

besides the hydrogens were treated anisotropically in **4b**. This difference in the refinement strategies between **4** and **4b** prevented us from comparing structural parameters related to the CO ligands, which have been shown to be greatly affected by the choice of the structural models.[24] Geometrical constraints were applied to the phenyl rings imposing equality on ortho, meta, and para C–C bonds. The H atoms of the phenyl and methyl groups were added in calculated positions [C–H = 1.08 Å] and refined "riding" on their respective C atoms.

Results and Discussion

Synthesis of $MIr_4(CO)_{10}(C_5Me_5)(PPh)$ [M = Rh (3), Ir (4)]. We recently reported the deprotonation reactions of the bright yellow compound $Ir_4(CO)_{11}(PPhH_2)$ (**1a**) with 1 equiv of DBU in acetonitrile or with 1 equiv of BuLi in THF, which afforded an extremely air- and moisture-sensitive dark-red anionic product (**1x**). Complex **1x** could not be isolated for full characterization, but IR and ^1H NMR spectroscopy suggested that this monoanion was not related to the phosphido species $[Ir_4(CO)_{10}(\mu\text{-}PPh_2)]^-$, obtained from the deprotonation reaction of $Ir_4(CO)_{11}(PPh_2H)$ under the same conditions. Furthermore, reaction of **1x** with another equivalent of base did not yield a dianionic species, and excess base led to only decomposition products.[16,25]

When the deprotonation of **1a** is carried out in acetonitrile with DBU in the presence of the dicationic species $[M(C_5Me_5)(NCMe)_3][SbF_6]_2$ (M = Rh or Ir), the dark-brown air-stable compound $MIr_4(CO)_{10}(C_5Me_5)(PPh)$ [M = Rh (**3**) or Ir (**4**)] is formed under mild conditions. Both these species are purified by TLC and formulated on the basis of FAB MS. The yields of the products are found to depend critically on the nature of the dication and the reaction conditions. Reaction with the Rh^{2+} species invariably gives better yields (above 85%) than with the Ir^{2+} compound (up to 50%). This is probably related to the fact that the reaction with the relatively more acidic Rh^{2+} species is readily achieved at room temperature, while the best yields of the pentairidium compound **4** are obtained when the condensation reaction is carried out at 50 °C, where decomposition of the monoanion **1x** is also fast. When the reaction with $[M(C_5Me_5)(NCMe)_3][SbF_6]_2$ (M = Rh or Ir) is carried out in dichloromethane, both **3** and **4** are obtained in yields less than 30%. In both cases, a number of other products are also formed, among which are **3x** and **4x**, which were purified by TLC and formulated on the basis of FAB MS as $RhIr_8(CO)_{20}(C_5Me_5)(PPh)_2$ and $Ir_9(CO)_{20}(C_5Me_5)(PPh)_2$, respectively (see Experimental Section).

Compounds **3** and **4** were fully characterized by analytical and spectroscopic methods (see Experimental Section). Their identical IR spectra in the ν_{CO} region, with bands due to terminal and bridging CO's, suggest a very similar solution geometry for both compounds. On the basis of Wade's rules, a square-based pyramidal metal framework is anticipated for the 74-electron clusters $MIr_4(CO)_{10}(C_5Me_5)(PPh)$ (M = Rh (**3**) and Ir (**4**)]. Two isomeric structures are possible, one with the "$M(C_5Me_5)$" fragment in an equatorial position (A) and another in the apical position (B). However, the latter structure was readily eliminated by a combination of ^1H and $^{31}P\{^1H\}$ NMR studies of the rhodium derivative **3**. A direct P–Rh interaction was suggested by the observation of a large $J_{P\text{-}Rh}$ (105.4 Hz) in the ^{31}P NMR spectrum and of $J_{H\text{-}P}$ (2.2 Hz) in the ^1H NMR spectrum, both favoring structure A. The molecular structure of **4** was fully characterized by X-ray analysis as described below.

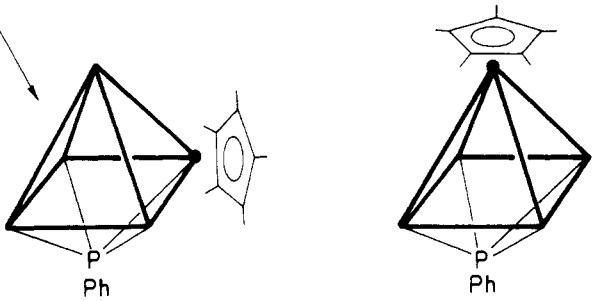

(A) (B)

Reactions of 3 and 4 with Tertiary Phosphines and Preparation of $MIr_4(CO)_9L(C_5Me_5)(PPh)$ [M = Rh, L = PPh_2Me (3a), PPh_3 (3b) and M = Ir, L = PPh_2Me (4a), PPh_3 (4b)]. Carbonyl substitution in **3** and **4** for tertiary phosphines to give $MIr_4(CO)_9L(C_5Me_5)(PPh)$ [M = Rh, L = PPh_2Me (**3a**), PPh_3 (**3b**); M = Ir, L = PPh_2Me (**4a**), PPh_3 (**4b**)], is easily achieved in two ways: (a) treatment of **3** or **4** with 1 equiv of Me_3NO in the presence of the desired ligand or (b) reaction of **3** or **4** with 1 equiv of Bu_4NBr in refluxing THF, to form an anionic compound $[MIr_4(CO)_9Br(C_5Me_5)(PPh)]^-$ [M = Rh (**3c**), Ir (**4c**), respectively], followed by bromide abstraction with $AgSbF_6$ in the presence of the desired ligand.

Attempts at direct CO substitution in **3** and **4** with PPh_3 in refluxing hexane resulted in only very low yields of **3b** and **4b**, respectively, together with decomposition products and unreacted starting material. Method a, via oxidative displacement of a CO ligand by Me_3NO, gives the highest yields (above 90%) and is the procedure of choice for the activation of **3** and **4**. Interestingly, method b, which has been used successfully for the synthesis of numerous $Ir_4(CO)_{12}$ derivatives,[18] affords only low yields of the products. The relative failure of this method may be related to the reluctance with which **3** and **4** react with Br^- compared with $Ir_4(CO)_{12}$ under the same reaction conditions.[20] The presence of the good π donor C_5Me_5 ligand in these clusters might be partly responsible for such behavior.

Compounds **3c** and **4c** were not isolated for full characterization. They were formulated on the basis of IR spectroscopy only, showing a characteristic shift of about 30 cm^{-1} to lower frequencies compared to **3** and **4**. The similarity of their spectra with that of the phosphine-substituted species also supports such a formulation.

Compounds **3a**, **3b**, **4a**, and **4b** were purified by TLC and fully characterized by analytical and spectroscopic methods (see Experimental Section). The dark-brown $RhIr_4$ species and the olive-green Ir_5 derivatives exhibit almost identical IR spectra in the ν_{CO} region and are believed to possess similar solution structures.

The three isomeric square-based pyramidal structures with ligand L either on one of the equatorial iridium atoms trans (structure C) or cis (structure D) to the "$M(C_5Me_5)$" fragment or on the apical iridium structure (structure E) could be proposed for these 74-electron clusters. The latter structure (E) was discarded on the basis of the $^{31}P\{^1H\}$ NMR spectrum of **3a**, which shows a 6.1-Hz coupling between phosphinidene and phosphine P nuclei. Although an equivalent coupling was not observed in the spectrum of **4a**, the ^1H NMR spectrum of both species confirmed this assignment, as the coupling between the methyl hydrogens of PPh_2Me and the phosphinidene phosphorus could be seen. Spectroscopic data alone did not distinguish

(24) Braga, D.; Koetzle, T. F. *J. Chem. Soc., Chem. Commun.* **1987**, 144.

(25) Khattar, R.; Raithby, P. R.; Vargas, M. D., manuscript in preparation.

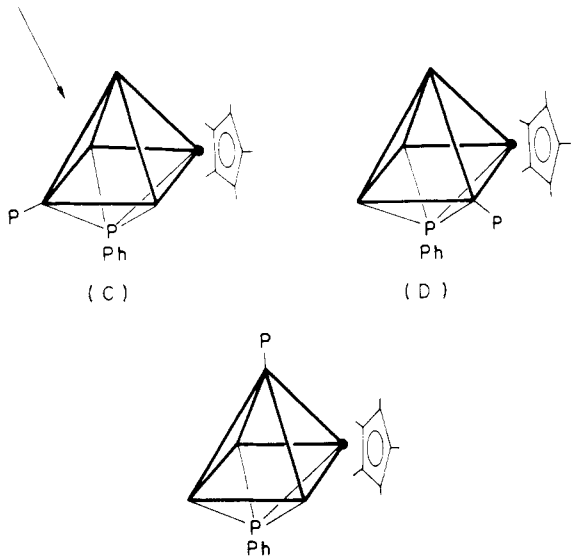

between configurations C and D, but a qualitative assessment of the most likely position for the nucleophilic attack in **3** and **4** pointed at the Ir atom trans to the "M-(C_5Me_5)" fragment, which is farthest away from the electron-rich C_5Me_5 ligand, indicating C as the most probable structural arrangement for these compounds. This ligand arrangement was confirmed by an X-ray structure analysis of **4b**, whose molecular structure is described below.

Compounds **3a**, **3b**, **4a**, and **4b** have also been obtained in relatively good yields (above 60%) by direct reaction of the tetranuclear disubstituted clusters $Ir_4(CO)_{10}(PPhH_2)L$ [L = PPh_2Me (**2a**) or PPh_3 (**2b**)] with the dications $[M(C_5Me_5)(NCMe)_3][SbF_6]_2$ (M = Rh, Ir) in the presence of DBU. Considering that **2a** and **2b** are themselves obtained in yields above 80% based on $Ir_4(CO)_{12}$,[17] the Ir_5 derivatives **4a** and **4b** are best synthesized following this route. A summary of all the synthetic routes to these species is presented in Scheme I.

The mechanism of the condensation reactions of **1** on one hand and **2a** and **2b** on the other hand is not clear. Under thermal conditions, cluster-bound ligands such as PH_3 and PRH_2 have been shown to undergo facile metalation via displacement of carbonyl or acetonitrile groups to yield clusters of the same or higher nuclearity. For example, $HOs_3(CO)_{10}(\mu\text{-}PPhH)$, obtained from $Os_3(CO)_{11}PPhH_2$, condenses under thermolytic conditions with fragments of $Os_3(CO)_{12}$ to give $Os_5(CO)_{15}(\mu\text{-}PPh)$.[11] In both types of condensation, the phosphorus ligand acts as an anchor directing the process. As suggested in Scheme II, the phosphorus ligand seems to play a key role in this process, first in the initial linking to the dications and second by holding the metal atoms together for a subsequent metal rearrangement to form the products. An indication for the directing role of this ligand is that among the two possible isomers of **3** and **4** and the three isomers of **3b** and **4b**, only one isomer is formed in each case.

Description of the Structures of $Ir_5(CO)_{10}(C_5Me_5)(PPh)$ (4) and $Ir_5(CO)_9(PPh_3)(C_5Me_5)(PPh)$ (4b). The molecular structures of **4** and **4b** have been established by single-crystal X-ray diffraction and are shown in Figures 1 and 2, respectively. The atomic coordinates for **4** and **4b** are reported in Tables II and III and relevant structural parameters in Tables IV and V, respectively. Because of their close relationship, the two molecular geometries will be discussed together. All structural parameters related to **4** will be reported in the following as mean values, averaged over pairs of corresponding values in the two independent molecules present in the asymmetric unit of **4** (see Experimental Section). Individual values for the two independent molecules are listed together in Table IV for comparison.

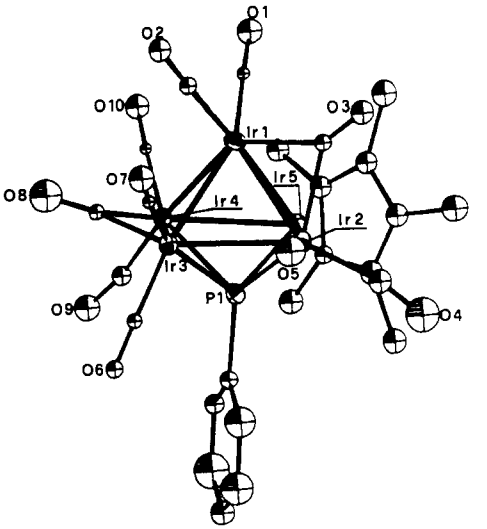

Figure 1. Molecular structure of $Ir_5(CO)_8(\mu\text{-}CO)_2(\eta^5\text{-}C_5Me_5)(\mu_4\text{-}PPh)$ (**4**).

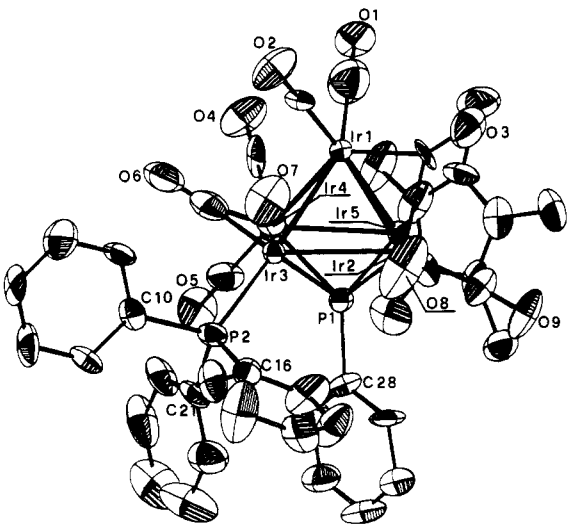

Figure 2. Molecular structure of $Ir_5(CO)_7(\mu\text{-}CO)_2(PPh_3)(\eta^5\text{-}C_5Me_5)(\mu_4\text{-}PPh)$ (**4b**).

Scheme I

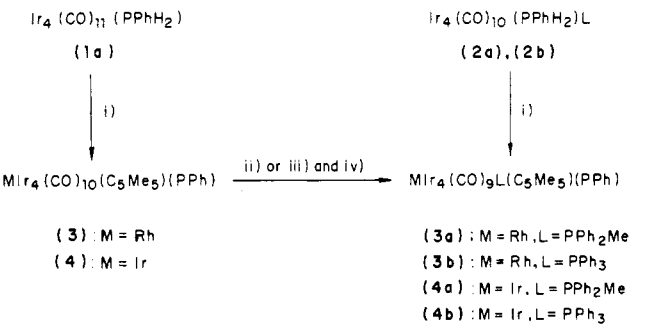

The five Ir atoms define a square-pyramidal metal atom framework. This is a novel stereochemistry for iridium

Scheme II

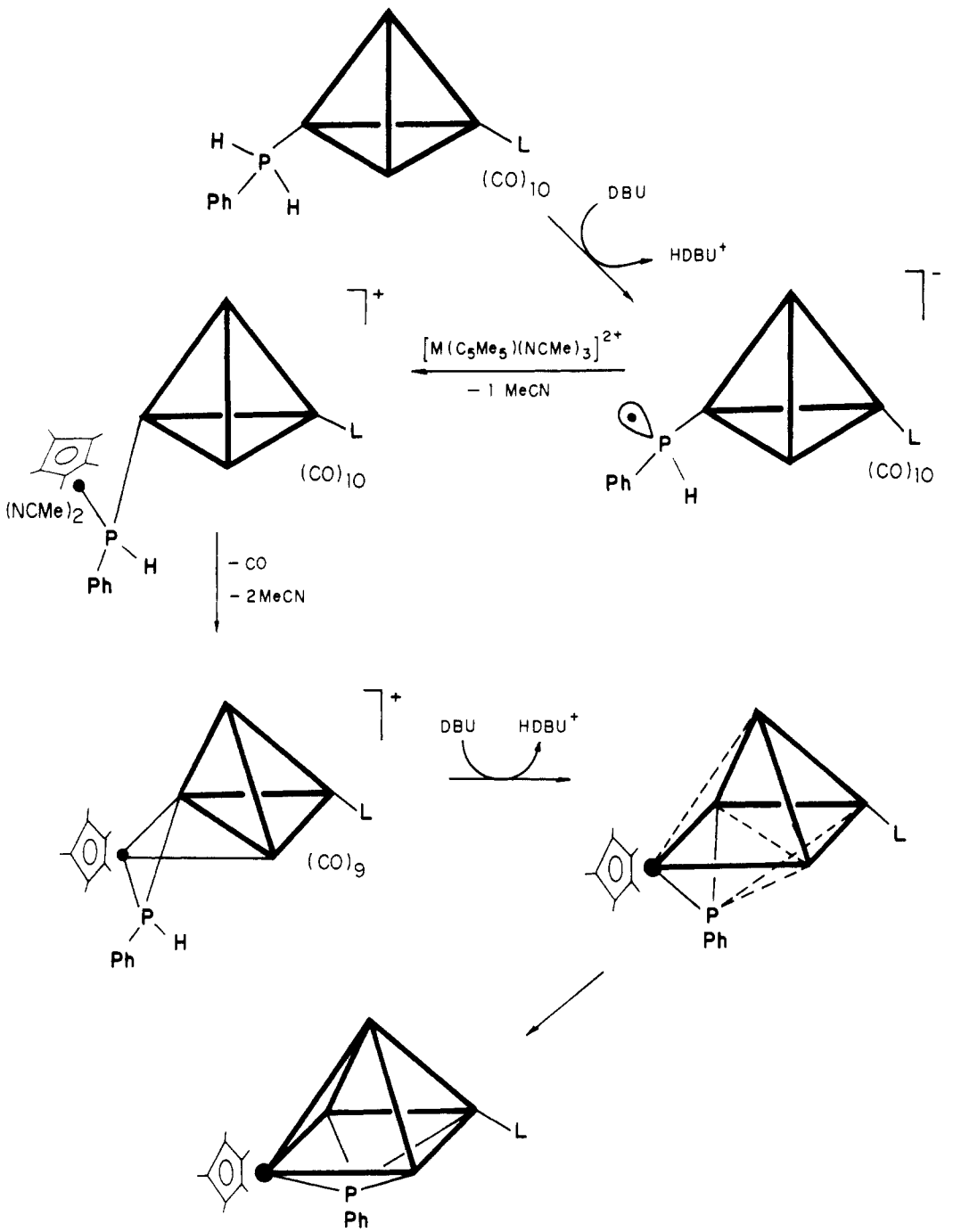

clusters, having so far been observed only in homometallic clusters of the iron subgroup[11,12] and in some mixed-metal clusters.[8,13] The square base of the Ir_5 core is supported by a μ_4-phosphinidene ligand. The basal Ir atom, which is not involved in CO interactions, bears a η^5-C_5Me_5 ligand, and the remaining Ir atoms are involved in two interactions with terminal CO's and one interaction with bridging CO's. The bridging carbonyl ligands span one basal edge and one noncontiguous apical edge of the metal framework in both **4** and **4b**. The main structural differences between the two species arise from the presence of the PPh_3 ligand in **4b**, which replaces an axial CO on the Ir atom trans to the Ir atom bearing a η^5-C_5Me_5 ligand. Considering formal five- and four-electron contributions from the C_5Me_5 and PPh ligands, respectively, the two species possess 74 electrons and are in agreement with the "magic number" of electrons observed for other square-pyramidal cluster species such as $M_5C(CO)_{15}$ [M = Fe, Ru, Os],[26] $[Os_5(CO)_{15}(\mu_4\text{-POMe})]$,[27] and $Os_5(CO)_{15}(\mu_4\text{-S})$.[28] Ir–Ir bond lengths fall in a narrow range [2.747 (1)–2.826 (1); 2.741 (1)–2.843 (1) Å in **4** and **4b**, respectively] with no detectable differences between Ir–Ir bonds spanned or not spanned by the bridging carbonyl ligands. This observation is in agreement with the general behavior exhibited by most Ir clusters when μ-CO's are present.[29] It is interesting to observe, however, that the basal Ir–Ir bonds are slightly longer than the apical ones [mean 2.789 (1), 2.762 (1) in **4**, 2.791 (1), 2.765 (1) Å

(26) (a) Braye, E. H.; Dahl, L. F.; Hübel, W.; Wampler, D. L. *J. Am. Chem. Soc.* **1962**, *84*, 4633. (b) Eady, C. R.; Johnson, B. F. G.; Lewis, J.; Matheson, T. *J. Organomet. Chem.* **1971**, *32*, C49. (c) Jackson, P. F.; Johnson, B. F. G.; Lewis, J.; Nicholls, J. N.; McPartlin, M.; Nelson, W. J. H. *J. Chem. Soc., Chem. Commun.* **1980**, 546.

(27) Fernandez, J. M.; Johnson, B. F. G.; Lewis, J.; Raithby, P. R. *J. Chem. Soc., Chem. Commun.* **1978**, 1015.

(28) Adams, R. D.; Horvath, I. T.; Segmüller, B. E.; Yang, L. W. *Organometallics* **1983**, *2*, 1301.

(29) Braga, D.; Grepioni, F. *J. Organomet. Chem.* **1987**, *336*, C9.

Table II. Fractional Atomic Coordinates for 4

atom	x	y	z	atom	x	y	z
Ir(1)	0.07720 (5)	0.28767 (5)	0.94120 (6)	C(19)	0.3143 (4)	0.1026 (9)	1.1163 (11)
Ir(2)	0.22514 (6)	0.21120 (5)	0.85112 (6)	C(20)	0.2874 (4)	0.1636 (9)	1.1872 (11)
Ir(3)	0.20230 (5)	0.39360 (5)	0.86225 (6)	C(21)	0.1907 (4)	0.1601 (9)	1.1955 (11)
Ir(4)	0.18665 (5)	0.38833 (5)	1.05791 (6)	C(22)	0.0598 (7)	0.0654 (10)	1.1233 (12)
Ir(5)	0.22187 (5)	0.20546 (5)	1.04954 (6)	C(23)	0.2305 (23)	−0.0187 (17)	1.0149 (21)
P(1)	0.2991 (3)	0.3019 (3)	0.9705 (4)	C(24)	0.4154 (14)	0.0771 (19)	1.0973 (21)
Ir(6)	0.68757 (6)	0.09921 (5)	0.53272 (6)	C(25)	0.3537 (19)	0.2131 (18)	1.2538 (19)
Ir(7)	0.79632 (6)	0.20747 (5)	0.64114 (6)	C(26)	0.1364 (17)	0.2131 (15)	1.2690 (16)
Ir(8)	0.60288 (6)	0.24256 (5)	0.62162 (6)	C(27)	0.7071 (18)	0.0165 (17)	0.4410 (19)
Ir(9)	0.60041 (5)	0.23524 (5)	0.42577 (6)	O(27)	0.7119 (18)	−0.0321 (17)	0.3812 (19)
Ir(10)	0.79397 (5)	0.21186 (5)	0.44122 (6)	C(28)	0.5982 (20)	0.0338 (19)	0.5876 (21)
P(2)	0.7138 (3)	0.3078 (3)	0.5298 (4)	O(28)	0.5525 (18)	−0.0170 (16)	0.6197 (18)
C(1)	−0.0054 (17)	0.2676 (16)	1.0309 (17)	C(29)	0.7957 (17)	0.0696 (16)	0.6236 (18)
O(1)	−0.0572 (15)	0.2485 (14)	1.0900 (15)	O(29)	0.8458 (15)	0.0119 (14)	0.6626 (16)
C(2)	−0.0191 (14)	0.3494 (13)	0.8676 (14)	C(30)	0.7834 (16)	0.2112 (15)	0.7750 (17)
O(2)	−0.0794 (14)	0.3883 (13)	0.8222 (14)	O(30)	0.7745 (14)	0.2201 (13)	0.8549 (14)
C(3)	0.0900 (15)	0.1736 (14)	0.8716 (15)	C(31)	0.9215 (16)	0.2327 (15)	0.6562 (16)
O(3)	0.0528 (13)	0.1143 (12)	0.8536 (14)	O(31)	0.9967 (14)	0.2469 (12)	0.6712 (14)
C(4)	0.2984 (17)	0.1062 (15)	0.8445 (17)	C(32)	0.5551 (17)	0.3423 (16)	0.6679 (17)
O(4)	0.3534 (14)	0.0478 (13)	0.8402 (14)	O(32)	0.5271 (18)	0.4197 (16)	0.6958 (18)
C(5)	0.2222 (13)	0.2293 (12)	0.7210 (14)	C(33)	0.5619 (22)	0.1803 (21)	0.7180 (23)
O(5)	0.2105 (15)	0.2391 (14)	0.6401 (15)	O(33)	0.5504 (20)	0.1303 (19)	0.7885 (21)
C(6)	0.2981 (13)	0.4510 (12)	0.8159 (13)	C(34)	0.5002 (18)	0.2097 (16)	0.5127 (18)
O(6)	0.3590 (15)	0.4864 (14)	0.7838 (15)	O(34)	0.4217 (14)	0.2003 (13)	0.5139 (15)
C(7)	0.1252 (20)	0.4216 (18)	0.7530 (21)	C(35)	0.5395 (20)	0.3302 (19)	0.3568 (21)
O(7)	0.0814 (14)	0.4344 (13)	0.6799 (15)	O(35)	0.4970 (17)	0.3770 (16)	0.3056 (18)
C(8)	0.1538 (16)	0.4844 (15)	0.9612 (16)	C(36)	0.5834 (20)	0.1520 (19)	0.3281 (21)
O(8)	0.1181 (14)	0.5543 (13)	0.9595 (14)	O(36)	0.5782 (12)	0.1039 (12)	0.2678 (13)
C(9)	0.2702 (20)	0.4464 (19)	1.1390 (21)	C(38)	0.6750 (11)	0.4798 (11)	0.4633 (11)
O(9)	0.3149 (20)	0.4979 (19)	1.1883 (21)	C(39)	0.6877 (11)	0.5689 (11)	0.4680 (11)
C(10)	0.0931 (13)	0.4018 (12)	1.1390 (14)	C(40)	0.7509 (11)	0.6006 (11)	0.5370 (11)
O(10)	0.0371 (15)	0.4072 (14)	1.1973 (15)	C(41)	0.8014 (11)	0.5432 (11)	0.6013 (11)
C(111)	0.4212 (10)	0.3188 (11)	0.9874 (13)	C(42)	0.7888 (11)	0.4540 (11)	0.5966 (11)
C(121)	0.4634 (10)	0.3355 (11)	1.0777 (13)	C(37)	0.7256 (11)	0.4223 (11)	0.5275 (11)
C(131)	0.5584 (10)	0.3458 (11)	1.0881 (13)	C(43)	0.8482 (8)	0.2741 (3)	0.3192 (8)
C(141)	0.6111 (10)	0.3394 (11)	1.0082 (13)	C(44)	0.9186 (8)	0.2641 (3)	0.3948 (8)
C(151)	0.5688 (10)	0.3227 (11)	0.9179 (13)	C(45)	0.9404 (8)	0.1735 (3)	0.4101 (8)
C(161)	0.4739 (10)	0.3124 (11)	0.9075 (13)	C(46)	0.8833 (8)	0.1274 (3)	0.3438 (8)
C(122)	0.4532 (10)	0.4013 (13)	1.0055 (41)	C(47)	0.8263 (8)	0.1896 (3)	0.2876 (8)
C(132)	0.5481 (10)	0.4122 (12)	1.0123 (35)	C(48)	0.7623 (21)	0.1769 (23)	0.1993 (18)
C(152)	0.5790 (10)	0.2579 (13)	0.9863 (39)	C(49)	0.8103 (17)	0.3594 (13)	0.2734 (17)
C(162)	0.4841 (10)	0.2486 (14)	0.9709 (33)	C(50)	0.9672 (16)	0.3386 (13)	0.4409 (16)
C(17)	0.1579 (4)	0.0969 (9)	1.1297 (11)	C(51)	1.0160 (16)	0.1301 (17)	0.4780 (18)
C(18)	0.2342 (4)	0.0614 (9)	1.0807 (11)	C(52)	0.8965 (21)	0.0304 (12)	0.3258 (22)

in **4b**]. Ir–Ir bond lengths agree in their overall mean values [2.776 (1), 2.778 (1) Å for **4** and **4b**, respectively] with the values reported for other high nuclearity Ir clusters such as $Ir_6(CO)_{16}$ ["red" isomer 2.779 (1), "black" isomer 2.778 (1) Å][30] and $[Ir_6(CO)_{15}]^{2-}$ [2.773 (1) Å],[31] but they are definitely longer than in $Ir_4(CO)_{12}$ [2.693 (7) Å][32] and in most of its derivatives.[29]

"Smoothing" of the electron distribution over the five metal centers is achieved through asymmetry of the bridging CO's [apical edge in **4** 1.99 (3), 2.13 (3), in **4b** 2.02 (2), 2.14 (2); basal edge in **4** 2.02 (3), 2.12 (3), in **4b** 2.02 (3), 2.12 (3) Å] and of the Ir–P (phosphinidene) interactions, which range from 2.250 (5) to 2.445 (5) Å in **4** and from 2.227 (6) to 2.436 (5) Å in **4b**. These latter interactions show their shortest value for the Ir atom bearing the C_5Me_5 ligand.

An interesting feature of the structures of **4** and **4b** is the position of the phenyl group belonging to the phosphinidene ligand. As mentioned above, **4** crystallizes with two independent molecules in the unit cell. Apart from small structural differences between the two independent molecules, which may be ascribed to differences in packing environment, the phenyl group is found to adopt three different orientations, as shown in Figure 3. While in molecule 1A the ligand is roughly parallel to a diagonal of the square base, in 1B the ligand is disordered (with 50% occupancy) over two alternative orientations related to that found in molecule 1A by ca. 30° rotation. We have checked and found that these latter orientations represent the maximum extent of rotation before the upsurge of re-

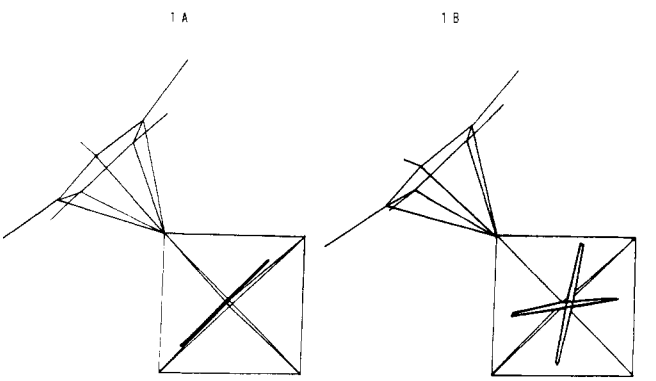

Figure 3. Schematic comparison of the phenyl group orientation in the two independent molecules of **4**. Left: molecule 1A, no disorder. Right: molecule 1B, 50% disorder over the two positions.

(30) Garlaschelli, L.; Martinengo, S.; Bellon, P. L.; Demartin, F.; Manassero, M.; Chiang, M. Y.; Wei, C. Y.; Bau, R. *J. Am. Chem. Soc.* **1984**, *106*, 6664.
(31) Demartin, F.; Manassero, M.; Sansoni, M.; Garlaschelli, L.; Martinengo, S.; Canziani, F. *J. Chem. Soc., Chem. Commun.* **1980**, 903.
(32) Churchill, M. R.; Hutchinson, J. P. *Inorg. Chem.* **1978**, *17*, 5328.

Table III. Fractional Atomic Coordinates for 4b

atom	x	y	z
Ir(1)	0.45597 (5)	0.26616 (9)	0.14807 (4)
Ir(2)	0.32690 (4)	0.25892 (9)	0.18320 (4)
Ir(3)	0.48049 (5)	0.25336 (9)	0.26236 (4)
Ir(4)	0.52258 (5)	0.04360 (9)	0.20884 (4)
Ir(5)	0.36846 (5)	0.03636 (9)	0.13428 (4)
P(1)	0.3966 (3)	0.0653 (6)	0.2249 (3)
P(2)	0.5090 (4)	0.2292 (7)	0.3560 (3)
C(1)	0.4875 (21)	0.2415 (42)	0.0877 (18)
O(1)	0.5058 (13)	0.2210 (26)	0.0481 (8)
C(2)	0.5136 (13)	0.4247 (20)	0.1625 (9)
O(2)	0.5491 (12)	0.5243 (19)	0.1715 (11)
C(3)	0.3451 (13)	0.3311 (29)	0.1098 (10)
O(3)	0.3044 (11)	0.3774 (21)	0.0717 (11)
C(4)	0.5817 (13)	0.0130 (28)	0.1601 (11)
O(4)	0.6198 (12)	−0.0016 (23)	0.1362 (10)
C(5)	0.5657 (16)	−0.1087 (31)	0.2474 (13)
O(5)	0.5917 (11)	−0.2084 (19)	0.2712 (10)
C(6)	0.5871 (15)	0.2041 (26)	0.2570 (11)
O(6)	0.6512 (10)	0.2364 (20)	0.2683 (8)
C(7)	0.4809 (15)	0.4371 (28)	0.2717 (11)
O(7)	0.4816 (12)	0.5523 (18)	0.2783 (10)
C(8)	0.6045 (13)	0.4171 (28)	0.2179 (11)
O(8)	0.2887 (13)	0.5049 (23)	0.2373 (13)
C(9)	0.2210 (14)	0.2120 (23)	0.1549 (13)
O(9)	0.1569 (9)	0.1854 (20)	0.1439 (9)
C(11)	0.6399 (9)	0.2468 (15)	0.4534 (6)
C(12)	0.7107 (9)	0.3013 (15)	0.4871 (6)
C(13)	0.7472 (9)	0.4031 (15)	0.4670 (6)
C(14)	0.7129 (9)	0.4504 (15)	0.4133 (6)
C(15)	0.6421 (9)	0.3959 (15)	0.3796 (6)
C(10)	0.6055 (9)	0.2941 (15)	0.3996 (6)
C(17)	0.3576 (10)	0.2905 (20)	0.3549 (8)
C(18)	0.3018 (10)	0.3555 (20)	0.3732 (8)
C(19)	0.3260 (10)	0.4488 (20)	0.4159 (8)
C(20)	0.4059 (10)	0.4770 (20)	0.4404 (8)
C(21)	0.4617 (10)	0.4119 (20)	0.4221 (8)
C(16)	0.4375 (10)	0.3187 (20)	0.3794 (8)
C(23)	0.4709 (11)	0.0153 (23)	0.4144 (8)
C(24)	0.4831 (11)	−0.1121 (23)	0.4379 (8)
C(25)	0.5406 (11)	−0.1954 (23)	0.4296 (8)
C(26)	0.5859 (11)	−0.1513 (23)	0.3979 (8)
C(27)	0.5738 (11)	−0.0239 (23)	0.3744 (8)
C(22)	0.5163 (11)	0.0594 (23)	0.3827 (8)
C(29)	0.2859 (8)	−0.0200 (14)	0.2707 (7)
C(30)	0.2496 (8)	−0.1072 (14)	0.2975 (7)
C(31)	0.2867 (8)	−0.2265 (14)	0.3198 (7)
C(32)	0.3600 (8)	−0.2587 (14)	0.3153 (7)
C(33)	0.3962 (8)	−0.1714 (14)	0.2885 (7)
C(28)	0.3592 (8)	−0.0521 (14)	0.2662 (7)
C(34)	0.3324 (18)	−0.0139 (27)	0.0435 (10)
C(35)	0.2639 (15)	−0.0036 (21)	0.0561 (12)
C(36)	0.2686 (13)	−0.0982 (27)	0.0990 (11)
C(37)	0.3419 (15)	−0.1763 (24)	0.1084 (10)
C(38)	0.3823 (16)	−0.1128 (34)	0.0759 (14)
C(39)	0.3412 (22)	0.0742 (43)	−0.0052 (13)
C(40)	0.1953 (18)	0.0831 (46)	0.0328 (14)
C(41)	0.2065 (16)	−0.1457 (36)	0.1253 (12)
C(42)	0.3707 (20)	−0.2907 (31)	0.1442 (13)
C(43)	0.4528 (15)	−0.1674 (36)	0.0629 (14)

pulsions (short intramolecular contacts) with either the axial CO's or the methyl groups of the C_5Me_5 ligand. We conclude that the PPh ligand has a limited rotational freedom and is allowed to "swing" below the square base between these limiting positions. [On these grounds it seems that the occurrence of a dynamic process, also in the solid state controlled by the packing environments around the two molecules, cannot be ruled out.]

For **4b** a substantially different situation is observed. Due to the presence of the bulky PPh_3 ligand in this molecule, the PPh group is now "locked" between the C_5Me_5 ligand and one phenyl group of the PPh_3, as shown in Figure 4. Evidence for the accommodation of relevant steric interactions between the PPh and PPh_3 ligands comes also from the bending of the Ph group with respect

Table IV. Selected Bond Distances (angstroms) and Angles (degrees) for 4 (with Estimated Standard Deviations in Parentheses)

Ir(1)–Ir(2)	2.758 (1)	Ir(6)–Ir(7)	2.752 (1)
Ir(1)–Ir(3)	2.798 (1)	Ir(6)–Ir(8)	2.784 (1)
Ir(1)–Ir(4)	2.747 (1)	Ir(6)–Ir(9)	2.754 (1)
Ir(1)–Ir(5)	2.738 (1)	Ir(6)–Ir(10)	2.764 (1)
Ir(2)–Ir(3)	2.806 (1)	Ir(7)–Ir(8)	2.817 (1)
Ir(3)–Ir(4)	2.758 (1)	Ir(8)–Ir(9)	2.735 (1)
Ir(4)–Ir(5)	2.826 (1)	Ir(c)–Ir(10)	2.801 (1)
Ir(2)–Ir(5)	2.775 (1)	Ir(7)–Ir(10)	2.790 (1)
P(1)–Ir(2)	2.414 (5)	P(2)–Ir(7)	2.392 (5)
P(1)–Ir(3)	2.385 (5)	P(2)–Ir(8)	2.396 (5)
P(1)–Ir(4)	2.429 (5)	P(2)–Ir(9)	2.445 (5)
P(1)–Ir(5)	2.250 (5)	P(2)–Ir(10)	2.241 (5)
Ir(1)–C(1)	1.83 (2)	Ir(6)–C(27)	1.83 (3)
C(1)–O(1)	1.20 (3)	C(27)–O(27)	1.12 (4)
Ir(1)–C(2)	1.83 (3)	Ir(6)–C(28)	1.90 (3)
C(2)–O(2)	1.17 (3)	C(28)–O(28)	1.17 (4)
Ir(1)–C(3)	2.01 (2)	Ir(6)–C(29)	1.98 (2)
Ir(2)–C(3)	2.12 (2)	Ir(7)–C(29)	2.13 (2)
C(3)–O(3)	1.11 (3)	C(29)–O(29)	1.21 (3)
Ir(2)–C(4)	1.88 (2)	Ir(7)–C(30)	1.89 (2)
C(4)–O(4)	1.16 (3)	C(30)–O(30)	1.14 (3)
Ir(2)–C(5)	1.83 (2)	Ir(7)–C(31)	1.88 (2)
C(5)–O(5)	1.14 (3)	C(31)–O(31)	1.13 (3)
Ir(3)–C(6)	1.85 (2)	Ir(8)–C(32)	1.78 (2)
C(6)–O(6)	1.18 (3)	C(32)–O(32)	1.30 (3)
Ir(3)–C(7)	1.86 (3)	Ir(8)–C(33)	1.81 (3)
C(7)–O(7)	1.17 (3)	C(33)–O(33)	1.28 (4)
Ir(3)–C(8)	2.09 (2)	Ir(8)–C(34)	2.14 (2)
Ir(4)–C(8)	2.01 (2)	Ir(9)–C(34)	2.01 (3)
C(8)–O(8)	1.16 (3)	C(34)–O(34)	1.16 (3)
Ir(4)–C(9)	1.87 (3)	Ir(9)–C(35)	1.88 (3)
C(9)–O(9)	1.24 (4)	C(35)–O(35)	1.13 (4)
Ir(4)–C(10)	1.83 (2)	Ir(9)–C(36)	1.88 (3)
C(10)–O(10)	1.19 (3)	C(36)–O(36)	1.12 (3)
P(1)–C(111)	1.81 (2)	P(2)–C(37)	1.78 (2)
mean C(Me)–C(Cp)	1.53 (1)	mean (Me)–C(Cp)	1.51 (1)
mean Ir(5)–C(Cp)	2.22 (1)	mean Ir(10)–C(Cp)	2.22 (1)
Ir(1)–C(1)–O(1)	175 (2)	Ir(6)–C(27)–O(27)	174 (2)
Ir(1)–C(2)–O(2)	179 (2)	Ir(6)–C(28)–O(28)	170 (3)
Ir(1)–C(3)–O(3)	142 (2)	Ir(6)–C(29)–O(29)	146 (2)
Ir(2)–C(3)–O(3)	134 (2)	Ir(7)–C(29)–O(29)	130 (2)
Ir(2)–C(4)–O(4)	171 (2)	Ir(7)–C(30)–O(30)	175 (2)
Ir(2)–C(5)–O(5)	173 (2)	Ir(7)–C(31)–O(31)	176 (2)
Ir(3)–C(6)–O(6)	178 (2)	Ir(8)–C(32)–O(32)	173 (2)
Ir(3)–C(7)–O(7)	174 (2)	Ir(8)–C(33)–O(33)	168 (3)
Ir(3)–C(8)–O(8)	137 (2)	Ir(8)–C(34)–O(34)	133 (2)
Ir(4)–C(8)–O(8)	138 (2)	Ir(9)–C(34)–O(34)	143 (2)
Ir(4)–C(9)–O(9)	168 (2)	Ir(9)–C(35)–O(35)	169 (3)
Ir(4)–C(10)–O(10)	175 (2)	Ir(9)–C(36)–O(36)	176 (3)
Ir(2)–P(1)–C(111)	127.0 (6)	Ir(7)–P(e)–C(7)	125.1 (6)
Ir(3)–P(1)–C(111)	119.6 (6)	Ir(8)–P(2)–C(7)	122.6 (6)
Ir(4)–P(1)–C(111)	120.8 (6)	Ir(9)–P(2)–C(7)	123.3 (6)
Ir(5)–P(1)–C(111)	126.6 (6)	Ir(10)–P(2)–C(7)	123.8 (6)

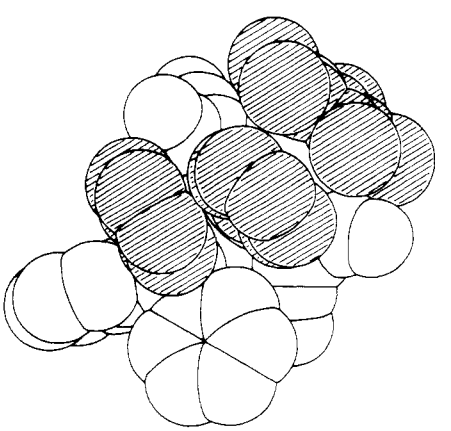

Figure 4. Space-filling diagram of **4b** showing the "locking" of the phenyl group of the μ_4-PPh ligand between the C_5Me_5 and the PPh_3 ligands.

to the μ_4-P–C axis (the angle between the Ph plane and the P–C bond is 174°) and from the short graphitic-like

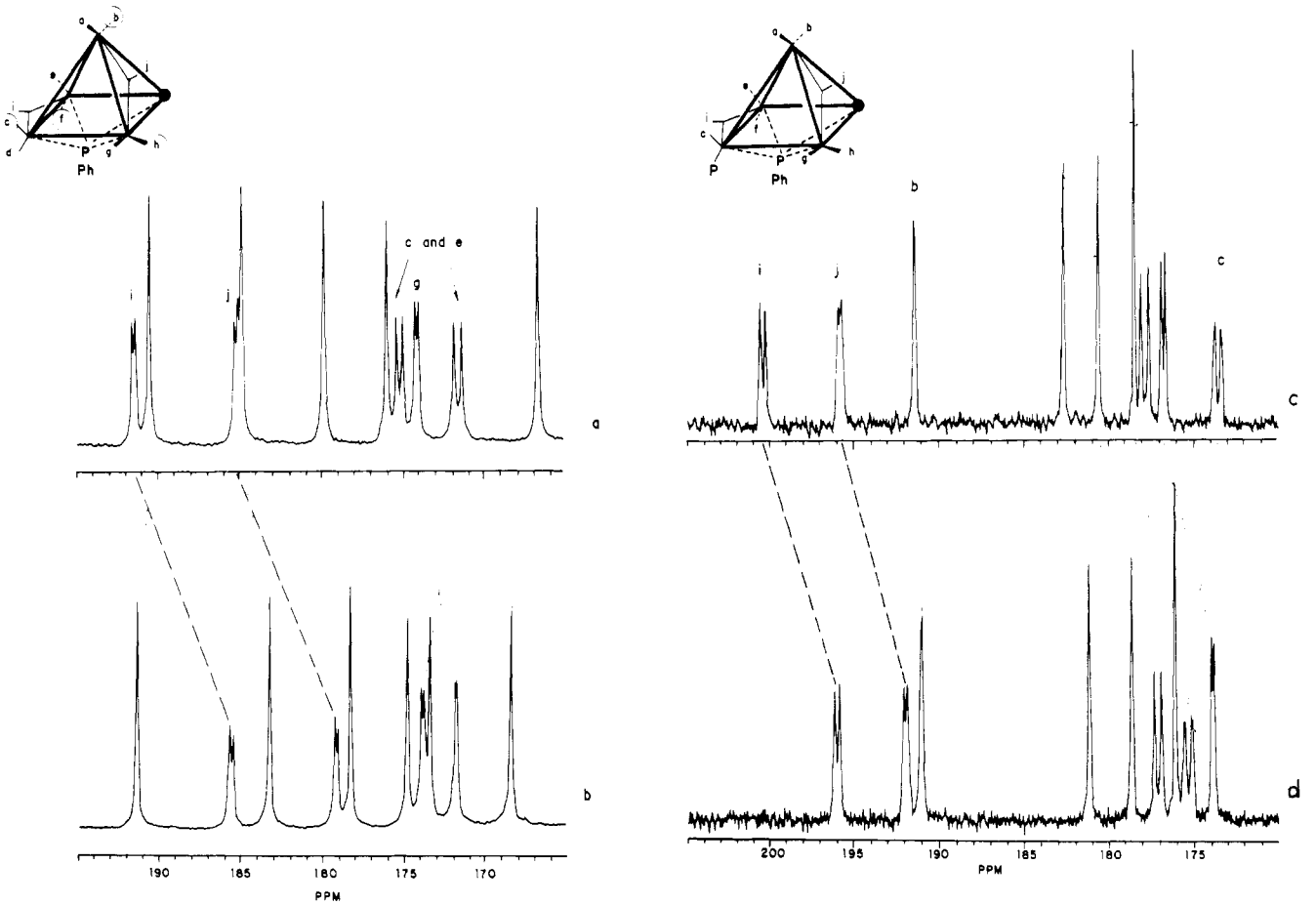

Figure 5. Limiting ^{13}C NMR spectra in the CO region of **3** at 183 K (a). **4** at 193 K (b), **3b** at 223 K (c), and **4b** at 205 K (d) in CD_2Cl_2, together with their schematic structures.

Table V. Selected Bond Distances (angstroms) and Angles (degrees) for 4b (with Estimated Standard Deviations in Parentheses)

Ir(1)-Ir(2)	2.745 (1)	C(4)-O(4)	1.06 (3)
Ir(1)-Ir(3)	2.817 (1)	Ir(4)-C(5)	1.84 (3)
Ir(1)-Ir(4)	2.756 (1)	C(5)-O(5)	1.18 (3)
Ir(1)-Ir(5)	2.741 (1)	Ir(3)-C(6)	2.02 (3)
Ir(2)-Ir(3)	2.843 (1)	Ir(4)-C(6)	2.12 (3)
Ir(3)-Ir(4)	2.742 (1)	C(6)-O(6)	1.14 (3)
Ir(4)-Ir(5)	2.806 (1)	Ir(3)-C(7)	1.85 (3)
Ir(2)-Ir(5)	2.772 (1)	C(7)-O(7)	1.16 (3)
P(1)-Ir(2)	2.364 (6)	Ir(2)-C(8)	1.92 (2)
P(1)-Ir(3)	2.406 (6)	C(8)-O(8)	1.09 (3)
P(1)-Ir(4)	2.436 (5)	Ir(2)-C(9)	1.86 (2)
P(1)-Ir(5)	2.227 (6)	C(9)-O(9)	1.12 (3)
P(2)-Ir(3)	2.297 (6)	P(2)-C(10)	1.85 (2)
Ir(1)-C(1)	1.83 (4)	P(2)-C(16)	1.82 (2)
C(1)-O(1)	1.18 (4)	P(2)-C(22)	1.81 (2)
Ir(1)-C(2)	1.86 (2)	P(1)-C(28)	1.85 (1)
C(2)-O(2)	1.16 (2)		
Ir(1)-C(3)	2.02 (2)	mean C(Me)-C(Cp)	1.51 (4)
Ir(2)-C(3)	2.14 (2)	mean C(Cp)-Ir(5)	2.23 (3)
C(3)-O(3)	1.11 (3)		
Ir(4)-C(4)	1.91 (3)		

Ir(1)-C(1)-O(1)	177 (3)	Ir(2)-P(1)-C(28)	122.8 (5)
Ir(1)-C(2)-O(2)	179 (2)	Ir(3)-P(1)-C(28)	124.4 (7)
Ir(1)-C(3)-O(3)	145 (2)	Ir(4)-P(1)-C(28)	124.8 (5)
Ir(2)-C(3)-O(3)	132 (2)	Ir(5)-P(1)-C(28)	120.9 (7)
Ir(4)-C(4)-O(4)	174 (2)	Ir(3)-P(2)-C(10)	116.2 (5)
Ir(4)-C(6)-O(6)	133 (2)	Ir(3)-P(2)-C(16)	110.5 (7)
Ir(3)-C(6)-O(6)	144 (2)	Ir(3)-P(2)-C(22)	117.1 (7)
Ir(3)-C(7)-O(7)	179 (2)	C(16)-P(2)-C(10)	104.6 (8)
Ir(2)-C(8)-O(8)	177 (2)	C(22)-P(2)-C(10)	99.3 (8)
Ir(2)-C(9)-O(9)	172 (3)	C(22)-P(2)-C(16)	108 (1)
Ir(4)-C(5)-O(5)	178 (3)		

interactions between the Ph(μ_4-PPh) and Ph(PPh_3) fragments (range 3.517–3.742 Å).

It is also noteworthy that the C_5Me_5 ligand does not have, in the solid, a rotational freedom comparable to the PPh system, being constrained between the neighboring radial CO's.

FAB and EI Mass Spectrometry. The FAB and EI mass spectrometry studies performed on compounds **3**, **4**, **3a**, and **4a** were essential for their formulation. EI MS gave satisfactory results of molecular weight in the case of compounds **3** and **4**; subsequent stepwise loss of 10 CO ligands was also observed. The EI MS of species **3a** and **4a** showed only peaks corresponding to $(M - 108)^+$ fragments together with ions resulting of the stepwise loss of nine CO's. This result suggests that the loss of the capping PPh group, not previously observed in analogous compounds,[10] may be occurring under the ionizing conditions. Characterization of **3a** and **4a** was successfully achieved by FAB MS, which also confirmed the molecular weight determination data obtained from EI MS for **3** and **4**. In all cases, positive ion spectra showing $(M + H)^{\bullet+}$ were observed. There are precedents where ions $(M + H)^{\bullet+}$ and even $(M + 2H)^{\bullet+}$ have been observed as a result of protonation by the matrix.[33] The fragmentation patterns observed for **3** and **4** are similar, with a stepwise loss of eight CO's, two less than in the EI MS, as a result of the softer ionizing conditions. Interestingly, the spectra of **3a** and **4a** show, in addition to the $(MH)^{\bullet+}$ fragment and sequential loss of CO groups, the $(MH - C_5Me_5)^{\bullet+}$ fragment and successive loss of three CO's from it.

^{31}P and ^{13}C NMR Spectroscopy. The limiting ^{13}C NMR spectra of **3** and **4** at 183 and 193 K, respectively,

(33) Blumenthal, T.; Bruce, M. I.; Shawkataly, O.; Green, B. N.; Lewis, I. *J. Organomet. Chem.* **1984**, *269*, C10.

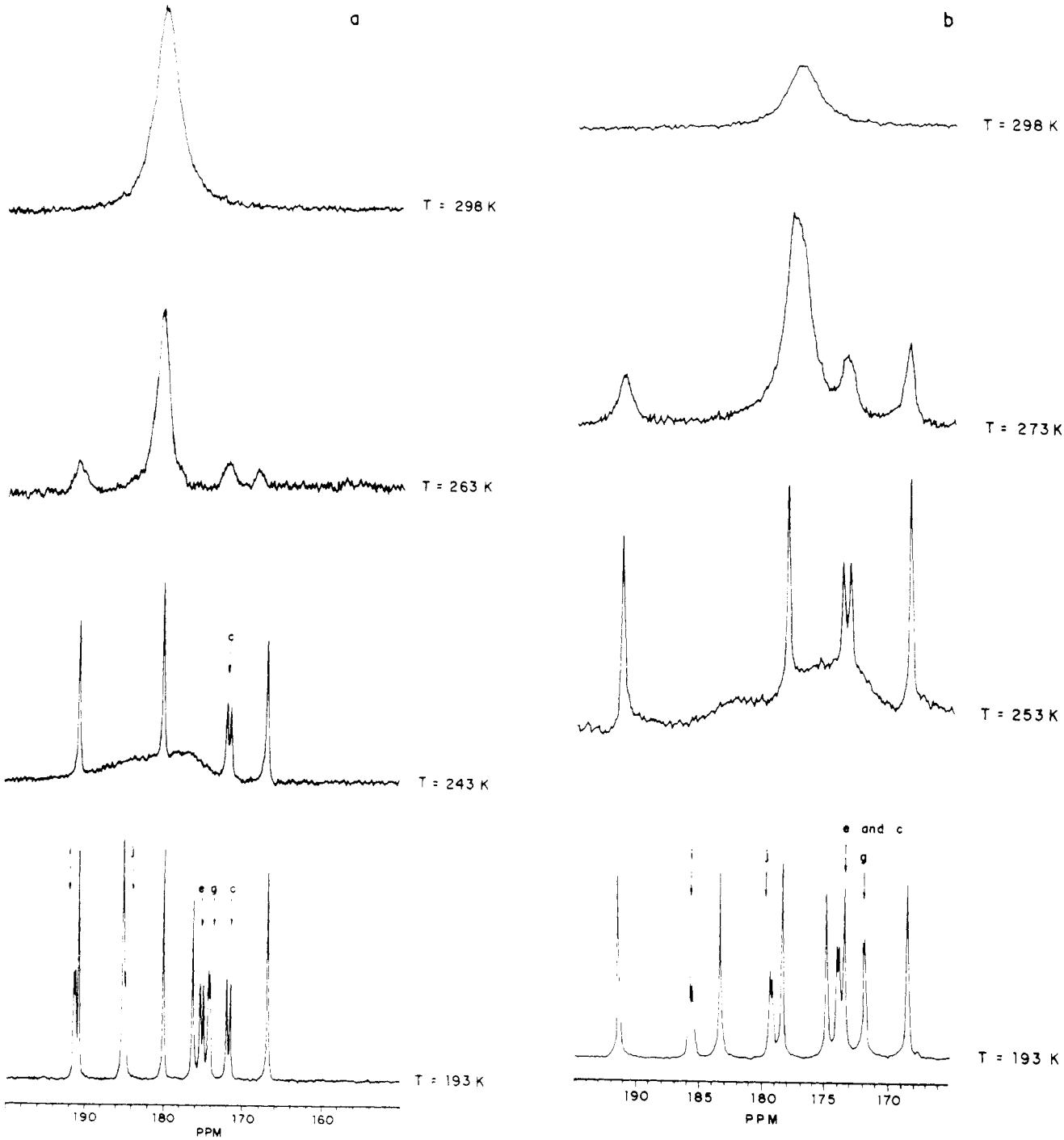

Figure 6. Variable-temperature ^{13}C NMR spectra of **3** (a) and **4** (b) in CD_2Cl_2.

in the CO region are rather similar, except for some small shifts in the CO resonances, which are discussed below (Figure 5). They exhibit five singlets and five doublets of equal intensity with the corresponding couplings of similar magnitude. The ^{13}C NMR spectrum of **3b** and **4b** at 223 and 203 K, respectively, are also similar and exhibit a doublet of doublets, five doublets, and three singlets of equal intensity (Figure 5). These data confirm that **3**, **4** and **3b**, **4b** respectively possess similar solution structures with all CO's inequivalent. No $^{103}Rh-^{13}C$ coupling was observed in the spectra of **3** and **3b**; the doublet resonances arose only from direct $^{31}P-^{13}C$ couplings.

At first sight the structures of these compounds in solution did not seem to be consistent with the solid-state structures determined for **4** and **4b**. Unlike the ^{13}C NMR spectra of metal carbonyl clusters containing σ-donor/π-acceptor ligands, for example, $Ir_4(CO)_{11}L$ (L = PEt_3,[34] PPh_2Me[35]), the spectra of compounds **3**–**4b** do not show a clearcut separation between terminal and bridging CO regions, raising the question of the actual presence of bridging carbonyls in these compounds in solution. To our knowledge, no ^{13}C NMR studies of square-based pyramidal clusters supported by a phosphinidene ligand have been reported to data, and ^{13}C NMR data on clusters containing the C_5Me_5 ligand are nonexistent. It is therefore rather difficult ot have a clear idea of the effects of both PPh and C_5Me_5 ligands on the chemical shifts of the carbonyls in these clusters. However, it is clear that for the compounds **3**, **3b**, **4**, and **4b** only a structure containing two bridging CO's and eight terminally bound ligands would have each

(34) Mann, B. E.; Spencer, C. M.; Smith, A. K. *J. Organomet. Chem.* **1983**, *244*, C17.
(35) Stuntz, G. F.; Shapley, J. R. *J. Am. Chem. Soc.* **1977**, *99*, 607.

of its metal atoms obeying the 18-electron rule. In addition, the solution IR spectra of these compounds clearly show bands in the bridging carbonyl region.

A comparative analysis of the ^{31}P NMR spectra of **3** and **4** and of their PPh_2Me derivatives **3a** and **4a** shows that in going from the $RhIr_4$ to the Ir_5 species, an upfield shift in the phosphinidene phosphorus resonance frequency occurs, which may be associated with the softer character of the Ir compared to the Rh atom. Bridging carbonyls would be expected to feel more strongly the electronic changes in the metal cage, which are associated with the substitution of Rh for Ir, than terminally bound CO's. This is supported by the fact that in either from **3** to **4** or from **3b** to **4b** (Figure 5), two doublet resonances are found to shift upfield significantly more than the others (shifts of 6.6, 7.0 and 5.6, 5.4 ppm, respectively) and are therefore assigned to the two bridging carbonyls i and j in these compounds. Minor upfield shifts were also noted in the resonances of the terminally bound CO's (average shift ca. 1.01 ppm). The resonances assigned to the bridging CO's in the spectra of **3b** and **4b** were those at lowest field as expected, but this was not found for compounds **3** and **4**. The two doublets at 191.42 and 185.15 ppm in **3** were shifted to 184.79 and 178.12 ppm in **4**, in the middle of the terminal CO resonances. Nevertheless, this assignment is strongly supported by the variable-temperature ^{13}C NMR studies discussed below.

Complexes 3 and 4. The limiting ^{13}C NMR spectra of **3** and **4** are fully consistent with the solid-state structure determined for **4** (Figure 1). A complete and unambiguous assignment of the 10 resonances observed in the spectra of both these compounds could not be achieved, due to the relatively low ^{13}CO enrichment, which prevented the observation of ^{13}C–^{13}C couplings. In addition to the two doublets assigned to the bridging CO's i and j, the other three doublets have been tentatively assigned to the radial carbonyls c and e (largest J_{C-P}) and to the radial almost basal carbonyl g, as all of them lie trans to the phosphinidene phosphorus.

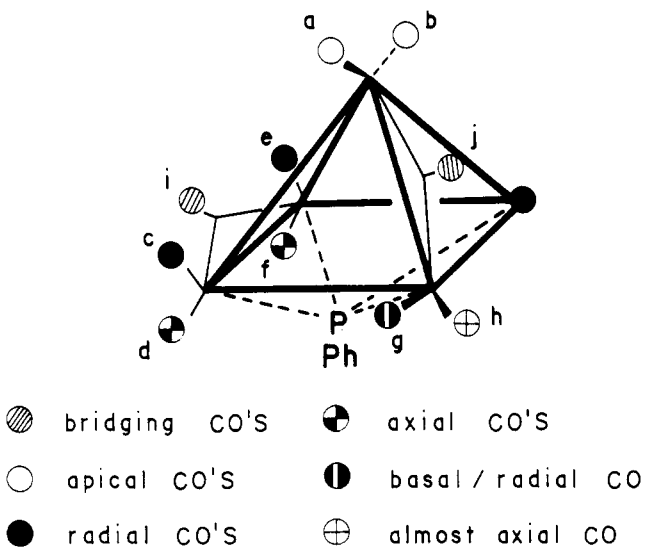

The ^{13}C NMR spectra of **3** and **4** at different temperatures are shown in Figure 6. As the changes observed are identical for both compounds, the discussion is restricted to the spectra of **4**, whose structure in the solid state is known. Gradually increasing the temperature from 193 to 243 K causes six resonances to broaden to the same extent and collapse, while the rest of the signals remain sharp. A further increase in the temperature to 273 K results in the broadening of the remaining four resonances

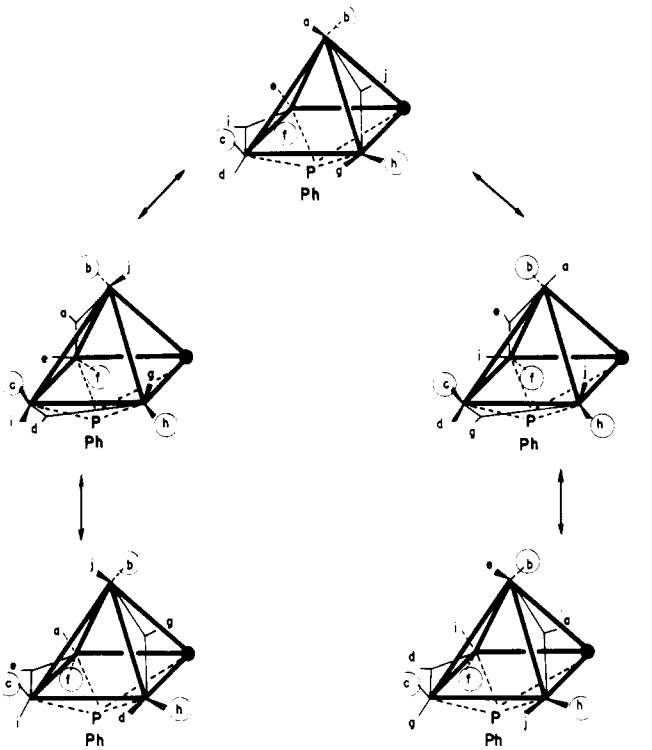

Figure 7. Possible mechanism for the initial CO equilibration in **3** and **4**.

and their coalescence to one peak at the weighted average at 298 K. These observations indicate that compounds **3** and **4** are involved in at least two types of fluxional processes. As shown in Figure 7 the first of these averaging processes may be explained by a site-exchange process involving the formation from the ground-state structure of its mirror image. In accord with the spectrum at 243 K one of the four ligands that do not enter into the averaging process shows a large J_{C-P}. This resonance could be assigned to carbonyl c, which is located on the hypothetical plane around which the rearrangement occurs. Two of the singlets are tentatively assigned to carbonyls f and h, which interconvert during the averaging process, and the third singlet to the apical carbonyl b.

The second fluxional process is observed at higher temperature and involves complete averaging of all carbonyls by a different process that is not yet definable.

Complexes 3b and 4b. Limiting ^{13}C NMR spectra of **3b** and **4b** suggest that the solid-state structure determined for **4b** is also maintained in solution. Thus, similar to the solid-state structure, all carbonyl positions are equivalent in the four compounds, with the exception of carbonyl d in **3** and **4** substituted for PPh_3 in **3b** and **4b**. A comparison of the ^{13}C NMR spectra of all these species is rather instructive and helps to assign the resonances in **3b** and **4b**. These tentative assignments will be discussed for **3b**, and the corresponding resonances for **4b**, suggested on the basis of the magnitude of the J_{C-P} values, are shown in Figure 5.

The spectrum of the CO-substituted species exhibits only two additional couplings due to the presence of the PPh_3 ligand observed in the resonances at 191.47 (d) and 173.54 (dd) ppm. Relatively large long-range coupling constants have been observed in the spectra of the tetrahedral clusters $Ir_4(CO)_{11}PPh_2Me$[35] for certain stereochemical relationships. When ligands are trans to each other in apical and axial positions, corresponding to situation $P–CO_b$ in **3b**, J_{b-P} = 24–25 Hz, when the ligands are trans to each other in an axial–radial position equivalent in **3b**

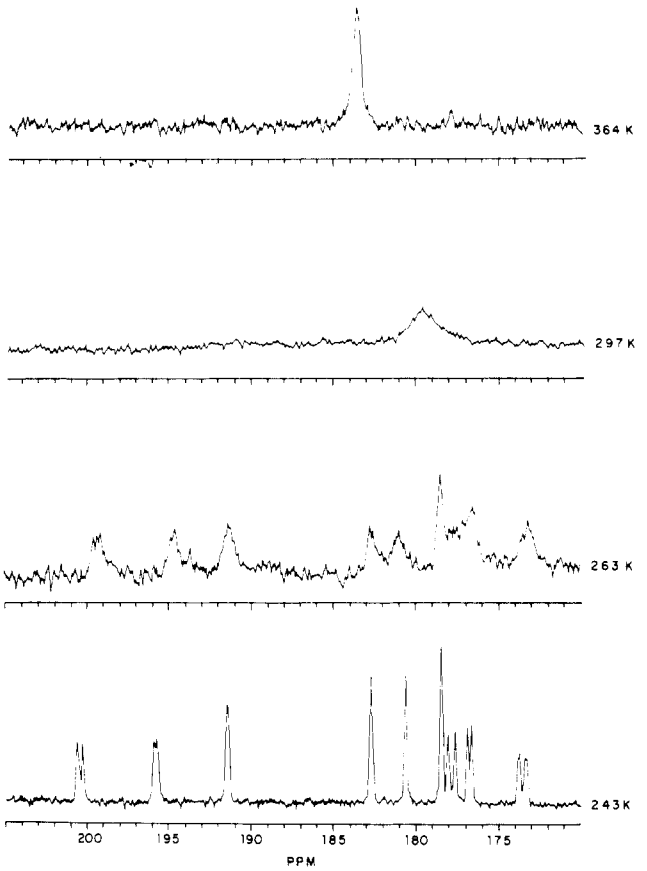

Figure 8. Variable-temperature ^{13}C NMR spectra of **3b** in CD_2Cl_2 (T = 243 and 263 K) and $C_2D_2Cl_4$ (T = 297 and 364 K) with $Cr(acac)_2$.

to P–CO_e, J_{e-P} = 14–15 Hz, and for ligands attached to the same iridium atom as in P–CO_c in **3b**, the coupling is weakest, $J_{C-P} \leq 9$ Hz. If this is valid for our compounds, the doublet at 191.47 ppm, J_{C-P} = 8.9 Hz, may be assigned to the apical carbonyl b, while the doublet of doublets at 173.54 ppm is most probably due to the axial carbonyl e, which would be coupling to the phosphinidene and to the phosphine P, J_{C-P} = 41.9 and 10.0 Hz, respectively, rather than to carbonyl c. The doublet at 177.82 ppm would therefore be assigned to carbonyl c, which couples strongly to the phosphinidene P, J_{C-P} = 44.5 Hz, but too weakly to the PPh_3 phosphorus to be observed. The last of the doublets at 176.74 ppm, J_{C-P} 22.8 Hz, is assigned to carbonyl g by exclusion. The three singlets are due to carbonyls a, h, and f.

The ^{13}C NMR spectra of **3b** at different temperatures are shown in Figure 8. Variable-temperature studies of **4b** were also performed and indicated a similar behavior, including the temperatures at which changes are observed. As the spectra obtained for **3b** were of much better quality, the discussion is restricted to this compound. The limiting spectrum remained unchanged from 193 to 243 K. At 263 K, all resonances broaden uniformly and coalesce into one broad band at 297 K. At 364 K averaging of all carbonyls occurs. With these spectroscopic data in hand it is rather difficult to speculate on the mechanistic aspects of CO exchange in these derivatives. However, a comparison of these NMR studies with those of **3** and **4** suggests that the substitution of a CO for PPh_3 ligand results in an increase in the energy barrier for the total CO exchange process, probably for steric reasons.

Acknowledgment. We thank Professor J. Lewis and Dr. B. F. G. Johnson for their help, encouragement, and extremely stimulating discussions throughout this work and for the use of all the facilities at the University Chemical Laboratories. We are grateful to Sidney Sussex College, Cambridge (UK), for a research fellowship (M. D.V.), the Nehru Trust for a research scholarship (R.K.), and the Ministero della Pubblica Istruzione (Italy) for financial support.

Supplementary Material Available: Complete listings of positional and thermal parameters, bond distances, and bond angles for **4** and **4b** (64 pages); listings of calculated and observed structure factors for **4** and **4b** (65 pages). Ordering information is given on any current masthead page.